Neuroscience Applied 3 (2024) 104075

Contents lists available at ScienceDirect

Neuroscience Applied

journal homepage: www.journals.elsevier.com/neuroscience-applied

Research Articles

Co-expression of prepulse inhibition and Schizophrenia genes in the mouse and human brain

Lillian Garrett [a,b,*], Dietrich Trümbach [b,*,‡], Donghyung Lee [p], Silvia Mandillo [o], Rodney Samaco [m,n,1], Ann M. Flenniken [l], Michelle Stewart [k], IMPC consortium, Jacqueline K. White [j], Colin McKerlie [q,w], Lauryl M.J. Nutter [q,r], Igor Vukobradovic [l], Surabi Veeraragavan [n], Lisa Yuva [n], Jason D. Heaney [n], Mary E. Dickinson [n], Hamid Meziane [s], Yann Hérault [s,t], Sara Wells [k], K.C. Kent Lloyd [u,v], Lynette Bower [v], Louise Lanoue [v], Dave Clary [v], Annemarie Zimprich [a,i], Valerie Gailus-Durner [a], Helmut Fuchs [a], Steve D.M. Brown [k], Elissa J. Chesler [j], Wolfgang Wurst [b,c,d,e,i], Martin Hrabě de Angelis [a,f,g], Sabine M. Hölter [a,b,h,i,*]

[a] Institute of Experimental Genetics and German Mouse Clinic, Helmholtz Zentrum München, German Research Center for Environmental Health, Neuherberg, Germany
[b] Institute of Developmental Genetics, Helmholtz Zentrum München, German Research Center for Environmental Health, Neuherberg, Germany
[c] TUM School of Life Sciences, Technische Universität München, Freising-Weihenstephan, Germany
[d] Deutsches Institut für Neurodegenerative Erkrankungen (DZNE) Site Munich, Feodor-Lynen-Str. 17, 81377, Munich, Germany
[e] Munich Cluster for Systems Neurology (SyNergy), Adolf-Butenandt-Institut, Ludwig-Maximilians-Universität München, Feodor-Lynen-Str. 17, 81377, Munich, Germany
[f] TUM School of Life Sciences, Technische Universität München, Alte Akademie 8, 85354, Freising, Germany
[g] German Center for Diabetes Research (DZD), Ingolstädter Landstr. 1, 85764 Neuherberg, Germany
[h] Technische Universität München, Freising-Weihenstephan, Germany
[i] German Center for Mental Health (DZPG), Partner Site, Munich, Germany
[j] The Jackson Laboratory, Bar Harbor, ME, USA
[k] Mary Lyon Centre, MRC Harwell, Harwell Campus, Oxfordshire, OX11 0RD, UK
[l] Lunenfeld-Tanenbaum Research Institute, The Centre for Phenogenomics, Toronto, ON, M5T 3H7, Canada
[m] Texas Children's Hospital, Jan and Dan Duncan Neurological Research Institute, Houston, TX, 77030, USA
[n] Baylor College of Medicine, Department of Molecular and Human Genetics, Houston, TX, 77030, USA
[o] Institute of Biochemistry and Cell Biology IBBC, National Research Council CNR, Via E. Ramarini 32, Monterotondo Scalo, Roma, 00015, Italy
[p] Department of Statistics, Miami University, Oxford, OH, USA
[q] The Hospital for Sick Children, Toronto, Canada
[r] The Centre for Phenogenomics, Toronto, ON, M5T 3H7, Canada
[s] Université de Strasbourg, CNRS, INSERM, Institut Clinique de La Souris (ICS), CELPHEDIA, PHENOMIN, 1 rue Laurent Fries, 67404, Illkirch, France
[t] Université de Strasbourg, CNRS, INSERM, Institut de Génétique et de Biologie Moléculaire et Cellulaire (IGBMC), 1 rue Laurent Fries, 67404, Illkirch, France
[u] Department of Surgery, School of Medicine, University of California Davis, and Mouse Biology Program, University of California Davis., California, USA
[v] Mouse Biology Program, University of California Davis, California, USA
[w] Department of Lab Medicine and Pathobiology, Faculty of Medicine, University of Toronto, Toronto, Canada

ARTICLE INFO

Keywords:
Schizophrenia
Prepulse inhibition
Endophenotype

ABSTRACT

Schizophrenia is a complex psychiatric disorder with genetic and phenotypic heterogeneity. Accumulating rare and genome-wide association study (GWAS) common risk variant information has yet to yield robust mechanistic insight. Leveraging large-scale gene deletion mouse phenomic data thus has potential to functionally interrogate and prioritize human disease genes. To this end, we applied a cross-species network-based approach to parse an

* Corresponding author. Institute of Developmental Genetics, Ingolstädter Landstr. 1, Helmholtz Center Munich, D-85764, Neuherberg, Germany.
E-mail address: sabine.hoelter-koch@helmholtz-munich.de (S.M. Hölter).
* These authors contributed equally.
‡ Present address: Institute of Metabolism and Cell Death, Helmholtz Zentrum München, German Research Center for Environmental Health, Neuherberg, Germany.
[1] Present address: Association of University Centers on Disabilities, Silver Spring, MD 20910, USA.

https://doi.org/10.1016/j.nsa.2024.104075
Received 22 November 2023; Received in revised form 7 May 2024; Accepted 3 June 2024
Available online 7 June 2024

Mouse models
Cross-species

extensive mouse gene set (188 genes) associated with disrupted prepulse inhibition (PPI), a Schizophrenia endophenotype. Integrating PPI genes with high-resolution mouse and human brain transcriptomic data, we identified functional and disease coherent co-expression modules through hierarchical clustering and weighted gene co-expression network analysis (WGCNA). In two modules, Schizophrenia risk and mouse PPI genes converged based on telencephalic patterning. The associated neuronal genes were highly expressed in cingulate cortex and hippocampus; implicated in synaptic function and neurotransmission and overlapped with the greatest proportion of rare variants. Concordant neuroanatomical patterning revealed novel core Schizophrenia-relevant genes consistent with the Omnigenic hypothesis of complex traits. Among other genes discussed, the developmental and post-synaptic scaffold *TANC2* (Tetratricopeptide repeat, ankyrin repeat and coiled-coil containing 2) emerged from both networks as a novel core genetic driver of Schizophrenia altering PPI. Aspects of psychiatric disease comorbidity and phenotypic heterogeneity are also explored. Overall, this study provides a framework and galvanizes the value of mouse preclinical genetics and PPI to prioritize both existing and novel human Schizophrenia candidate genes as druggable targets.

1. Introduction

Schizophrenia (SZ) is a complex and phenotypically heterogeneous psychiatric syndrome that contributes significantly to the global burden of disease (Solmi et al., 2023; Velligan and Rao, 2023a). Diagnosed by late adolescent/young adult onset of positive (e.g., auditory hallucinations, delusions) and negative (e.g., social withdrawal and anhedonia, blunted affect) symptoms (Velligan and Rao, 2023b), the latter is less responsive to currently available pharmacotherapies (Correll and Schooler, 2020). The limited understanding of the disease's molecular foundations has hampered improved treatment development.

Elucidating the SZ genetic architecture has the power to yield etiological insight. This disease is highly heritable (estimates as high as 81%) (Sullivan et al., 2003) and strongly polygenic. Common genetic variants (minor allele frequency >1%) make a significant heritability contribution (~24%) and genome wide association studies (GWAS) so far identified 287 common risk loci (Loh et al., 2015; Schizophrenia Working Group of the Psychiatric GenomicsC, 2014; Trubetskoy et al., 2022). Nevertheless, several rare chromosomal copy number variants (CNVs) represent an even greater disease risk (Marshall et al., 2017; Rees et al., 2014). Causal variant identification in CNVs and GWAS loci is complicated due to the presence of often multiple gene variants in high linkage disequilibrium (LD). Thus, analysis of rare coding variants, as the most immediate link between a genetic perturbation and disease pathogenesis, can provide molecular insight and aid in common variant mapping. While 10 exome-wide significant SZ-related ultra-rare coding variants (URV) were identified recently (Singh et al., 2022), unearthing additional URVs is hampered by low population frequency. Thus, approaches that can aid in identifying such rare variants can form the foundation for mechanistic insights and GWAS variant prioritization.

The Research Domain Criteria (RDoC) framework espouses the use of objective biological disease biomarkers to improve neuropsychiatric disease (NPD) diagnosis (Insel et al., 2010). In this context, endophenotypes are a quantifiable subtype more proximal to the disease genetic susceptibility (Cannon and Keller, 2006). Prepulse inhibition (PPI) of the acoustic startle reflex is a SZ-associated endophenotype (Mena et al., 2016; Swerdlow and Light, 2018). This operational measure of sensorimotor gating is the ability of a non-startling "prepulse" to temper the reflex response to a startling stimulus or "pulse" (Swerdlow et al., 2000). PPI is evolutionarily conserved, facilitating cross-species translational comparisons in preclinical genetic models to reveal novel and hence SZ-relevant genes (Powell et al., 2009). Of note, however, it is not Schizophrenia-specific and not all disrupted disease genes alter PPI in mice (Powell et al., 2009). Moreover, it is not clear how PPI aligns with SZ positive/negative symptoms and rare/common variants or how to parlay genetic risk into novel disease-gene identification.

The International Mouse Phenotyping Consortium (IMPC) has the potential to inform SZ understanding. This large-scale resource of protein-coding gene knockout (KO) mice and standardized multisystemic functional phenomic data (Brown and Moore, 2012) houses an extensive library of PPI-related genes. Our goal was to exploit this data (from 4031 genetic deletion models) to functionally interrogate and prioritize Schizophrenia rare and GWAS common signals. To this end, we applied a computational approach with the Omnigenic model (Sabik et al., 2021), the systems biology equivalent of the polygenic theory (Boyle et al., 2017). It posits that all genes expressed in a disease-relevant tissue (i.e. the brain for Schizophrenia) contribute to complex disease. Nevertheless, "core" genes directly influence a key disease endophenotype (e.g. rare variants affecting PPI) while "peripheral" genes affect core gene expression (Boyle et al., 2017; Sabik et al., 2021; Sabik et al., 2020). We used cross-species methods to parse the PPI genes into subnetworks. For this, we integrated mouse gene-KO PPI data (IMPC); common and rare variant Schizophrenia genes (GWAS catalog) and high-resolution mouse and human brain transcriptome (Allen Brain Atlas ABA) to identify a module of core established and novel genes as potential SZ-relevant genetic drivers and druggable targets (van Dam et al., 2018).

2. Methods

2.1. Mice

KO mouse lines in this study were derived from International Knockout Mouse Consortium (IKMC) ES cell resources or by CRISPR/Cas9 mutagenesis. All mice were produced and maintained on a C57BL/6N genetic background of sub-strains C57BL/6NJ, C57BL/6NTac or C57BL/6NCrl. Details on the production of each mouse line can be found at www.mousephenotype.org by searching by gene name. Husbandry practices vary between centers and details can be found at www.mousephenotype.org/impress. All procedures were conducted in compliance with ethical animal care and use guidelines at each center and in accordance with ARRIVE guidelines (https://www.mousephenotype.org/about-impc/animal-welfare/arrive-guidelines).

2.2. Study design

An overview of the study design is depicted in Fig. 1. We applied a two-pronged approach to identify Schizophrenia-relevant core gene modules from both human WGCNA and hierarchical clustering of mouse brain transcriptome respectively.

2.3. Phenotyping

The IMPC phenotyping pipeline consists of 14 mandatory and other optional tests that assess major biological systems and disease areas (www.mousephenotype.org). For each mouse line, 7 male and 7 female mutant mice were phenotyped from 4 to 16 weeks of age including age-matched, wild type C57BL/6N baseline controls. Homozygous male and female animals were phenotyped for mouse lines that were homozygous viable. Mouse lines were designated as sub-viable if they had fewer than 12.5% homozygous pups after intercross and production of a minimum of 28 pups (i.e., <50% of the expected 25%) while those with 0%

homozygous pups after intercross were designated lethal lines. Heterozygous male and female mice were phenotyped for both sub viable and lethal lines with the addition of surviving homozygous mice for subviable lines.

Within the IMPC pipeline, four mandatory and five optional behavior-specific tests were performed: mandatory tests were open field, combined SHIRPA and dysmorphology, grip strength, acoustic startle/prepulse inhibition, optional tests include holeboard exploration, light-dark box, fear conditioning, tail suspension, and rotarod (https://www.mousephenotype.org/impress/index). For all behavioral tests, animals could acclimatize to the phenotyping room in their home cage for at least 30 min before testing. Upon the test's completion, the animals were placed back in their home cage and returned to the housing room. All efforts were made to minimize animal discomfort by considerate housing, husbandry, and phenotyping methodology. Animal welfare was assessed routinely for all mice involved. Detailed description of all phenotyping tests is available on the IMPC website www.mousephenotype.org including all parameters and metadata.

2.4. Acoustic startle (S)/Prepulse inhibition (PPI)

The acoustic startle response is characterized by an exaggerated flinching response to an unexpected strong auditory stimulus (pulse). This response can be attenuated when it is preceded by a weaker stimulus (pre-pulse). PPI has been described in numerous species, including mice and humans and provides an operational measure of sensorimotor gating reflecting the ability of an animal to successfully integrate and inhibit sensory information. The experimental apparatus consists of an outer sound attenuated chamber in which an animal holder is mounted on a regularly calibrated load cell platform that records the startle response, linked to the transducer and amplifier. The test session is initiated with a 5 min acclimatization period (background noise, BN is ca. 65–70 dB) and, as an option, to the startle pulse alone for 5 times (excluded from the statistical analysis). The session is then continued by presentations of different trial types, each presented 6–10 times in a pseudorandom order, with an inter-trial interval (ITI) varying randomly between 20 and 30 s. The trial types are a) pre-pulse trials (PP1, PP2, PP3, PP4) of 10–20 ms duration and different intensities presented alone or that precede the startle pulse (PP–S) by 50–120 ms. The intensities of the pre-pulse are 2–20 dB above the background noise (BN) so that they do not elicit a significant startle response on their own; b) Startle pulse trials where 110–120 dB/40–60 ms of white noise is presented alone; c) No stimulus (NOSTIM) trials in which only background noise is presented to measure baseline movement of the animal. Startle response is recorded every millisecond for 65–100 ms after the onset of stimulus. The maximal peak amplitude is used to determine the acoustic startle response. Basal startle responses S and PP-S are calculated respectively as the average responses to the pulses presented alone and the average responses to the combined pre-pulse-pulses. The amount of pre-pulse inhibition (PPI) is calculated as a percentage score for each PP trial type: % PPI = 100 x (S –PPI-S)/S. The global level of PPI is also calculated as the mean % PPI for the different prepulse responses: 100 x [S – (PP1–S + PP2–S + PP3–S + PP4–S)/4]/S.

2.5. Data QC

Data generated by the IMPC partner centers were uploaded to the Data Coordination Center (DCC) where quality control and preliminary statistical analyses were performed. Initially, as part of the data upload process, data were validated against the IMPReSS and iMits resources to ensure accuracy and completeness of uploaded data. At this stage, validation checks were primarily concerned with ensuring data were formatted correctly and that a complete set of data including metadata was captured. Following the initial validation stage, data were inserted into a database at the DCC where they underwent further quality control procedures. During this stage, the data were checked for values out of established ranges and unexpected relationships between parameters. Stability and variability of phenotypic measures were also inspected visually. Changes in the distribution of data and deviation from normality (QQ plot and histograms) were noted as potential quality control issues and were then communicated with the data generating centers. Data was corrected by the center if technical issues were discovered. If the data-generating center determined that there was no reason to exclude data, then no changes were made. Examples of issues found during this stage included duplicate measurements, measurements with incorrect units, out of range measurements, miscalculations, and improper upload to IMPC.

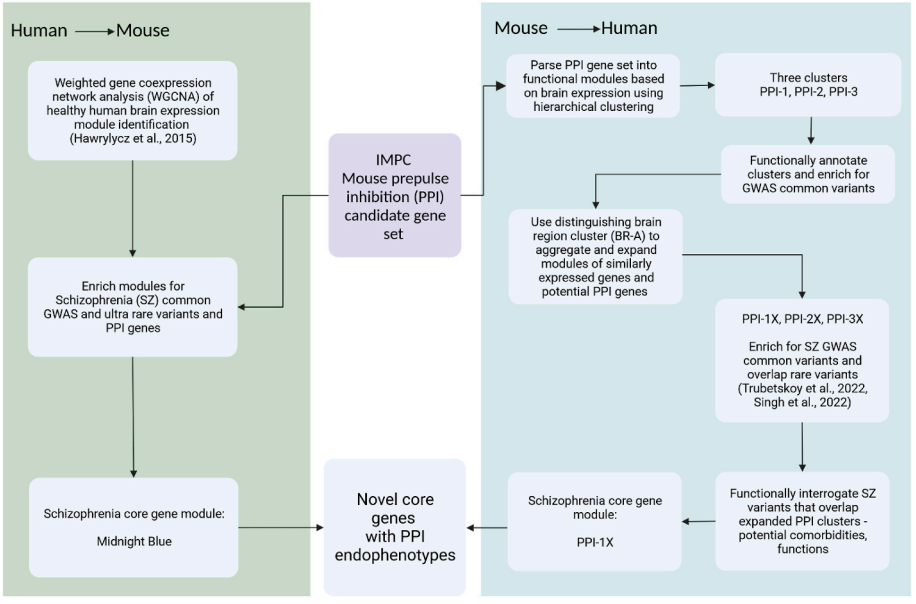

Fig. 1. Study overview using mouse prepulse inhibition (PPI) genes and brain expression to stratify human Schizophrenia common and ultra-rare variants and identify potentially novel ultra-rare variant genes with „core"-like properties. Created with BioRender.com.

2.6. Statistical analysis

The categorical data from the nominated behavioral lines were analyzed with two-tail Fisher's exact test whereas the continuous data were analyzed with the linear mixed-model, two of them implemented in the R software (R Team Core, 2017) and the package PhenStat version 2.18.010. Because IMPC data has been collected for over 10 years, the control data show heterogeneity that can be a result of seasonal effects, personnel changes, and other environmental factors. To reduce this heterogeneity, we utilized SoftWindowing introduced in (Haselimashhadi et al., 2020) and implemented in the R package SmoothWin (http://CRAN.R-project.org/package=SmoothWin) prior to applying the linear mixed model to the continuous measurements. This assigned non-increasing weights, ranging from 0 to 1, to control data subject to their distance in time from the mutants. That is, controls that are measured at or near the date of mutants are assigned the maximal weights whereas the ones at earlier or later dates are given less weights. Then the PhenStat is modified to apply the weighted linear mixed model (WLMM) using weights from the SoftWindowing approach (documentation BioConductor (https://www.bioconductor.org/packages/release/bioc/html/PhenStat.html). Prior to applying the default model selection in the PhenStat using backward elimination, the WLMM incorporated Genotype, Sex, Genotype-Sex interaction and body weight in the fixed effect term and Batch, defines as the date of experiment, in the random effect. All lines were processed using the two methods described above, but some with no variation in response were manually assigned a p-value of 0.999999. The raw data from the IMPC data release (DR) 10.1 (data release used for the current analysis), statistical pipeline and the statistical results are available from the IMPC FTP endpoint link (ftp://ftp.ebi.ac.uk/pub/databases/impc). At the time point of writing, the IMPC is currently using DR19.1 with 8483 KO genes phenotyped. As data has continually been added to the IMPC resource, the data available with each DR varies.

2.7. Multiple testing

The resulting p-values were corrected using the positive false discovery rate (pFDR) correction to create q-value.

2.8. Calculation of META SCORES

Cross-phenotype meta-analysis was conducted using gene-knockout-to-phenotype association summary statistics. Consider N-different mouse phenotypes like endophenotypes of a certain human disease. For each phenotype, assume that M different gene-knockouts were phenotyped, tested for gene-knockout-to-phenotype association and obtained association Z-scores (genotype beta-coefficient divided by its standard error). To simplify this, let Zij be an association Z-score for the ith gene and jth phenotype, $Z_i = \{Zi1, Zi2, Zi3, \ldots ZiN\}T$ and let Z represent a M × N matrix of Z-scores. Under the null hypothesis of no association between gene-knockout and phenotype, we assume that Zi follows a multivariate normal distribution with zero mean equal to 0 and covariance matrix Σ.

[**Step 1**] Estimate Σ, genetic correlations between phenotypes, by computing *cor(Z)*.

[**Step 2**] For ith gene, conduct a cross-phenotype meta-analysis:

[**Step 2-1**] Obtain a meta-score by computing $T_{obs} = \sum_{j=1}^{N} Z_{ij}^2$.

[**Step 2–2**] Simulate K vectors of Z-scores using a multivariate normal distribution with mean 0 and cor(Z).

[**Step 2–3**] Generate an empirical null distribution of the metascore test statistic by computing $(T_k^o, k = 1, \ldots K)$ for $\boldsymbol{K}$ simulated Z-score vectors.

[**Step 2–4**] Compute an empirical p-value by counting the number of times the null statistic T_k^o exceeds the observed one T_{obs} divided by the number of simulations (**K**).

[**Step 3**] Obtain multiple-testing adjusted p-values (q-value) using Benjamini-Hochberg procedure.

2.9. Hierarchical clustering analysis of PPI gene-related brain transcriptomic data

In situ hybridization (ISH) raw data, i.e., expression energies and corresponding brain tissues, was downloaded for 188 PPI genes from Allen Mouse Brain Atlas (ABA) (Data Release, October 4, 2018) via the Allen Brain Atlas application programming interface (API) (brain-map.org/api/index.html) by using custom-written bash scripts (Lein et al., 2007). They consisted of ISH data for 1707 different mouse brain regions in sagittal sections whereby developing mouse brain regions were excluded. We then performed a global unsupervised hierarchical clustering analysis as described previously (Garrett et al., 2023). For the generation of the heat map, we used the heatmap.2 function within the gplots package of R statistical software (www.r-project.org). Agglomerative hierarchical clustering by the hclust function (method = "ward.D2") was applied to group mouse brain regions (columns) as well as expression energies of genes (rows) for the heat map. Rows were scaled and represented as z-score. Blue indicates higher expression levels and yellow lower levels within the heat map. A dendrogram was shown for the columns (brain regions) and rows (genes), where the main subtrees were highlighted with letters (Fig. 3A). We used the silhouette method by the function fviz_nbclust from the R package factoextra to cut the dendrogram and determine the optimal number of clusters.

2.10. Human brain weighted gene co-expression network analysis (WGCNA)

The WGCNA network used in this study is from and described in detail in (Hawrylycz et al., 2015) and the Supplementary Data Set 1 and 2 therein. This study used the data from six healthy human donor brains available in the Allen Human Brain Atlas (http://human.brain-map.org/) interrogating samples from approximately 500 anatomically discrete regions for genome-wide gene expression using an Agilent 8 × 60K cDNA array chip. For all pairs of genes, a Pearson's correlation was calculated, and a signed similarity (Sij) parameter was derived. In the signed network, the gene similarity reflects the sign of the expression profile correlation. A signed network was constructed that summarized gene expression across 132 brain structure subsets for each brain. For the six individual donor brain networks, a consensus network was used to identify the common expression patterns. Genes were hierarchically clustered and module assignments were determined and merged until all pairs of module Eigen genes were correlated with $R < 0.8$ (for details see in online methods 'WGCNA consensus network construction' in (Hawrylycz et al., 2015). Finally, all 17348 expressed genes were assigned to modules based on kME. Module Eigen genes were calculated using all available data.

2.11. Functional and disease enrichment analysis of modules

To functionally annotate the PPI and WGCNA gene modules, and to determine disease associations, we performed enrichment analyses using the ENRICHR web interface focusing on gene ontology (GO) processes, mammalian phenotypes and diseases: MGI mammalian phenotype Level 4 2021, GO Biological processes, Reactome, SynGO and DisGeNET (Chen et al., 2013; Kuleshov et al., 2016; Xie et al., 2021). The Functional Mapping and Annotation of Genome-Wide Association Studies (FUMA) interface (Watanabe et al., 2017; Watanabe et al., 2019) was used to assess the spatio-temporal exonic expression during human development from the BrainSpan atlas and human tissue-specific gene

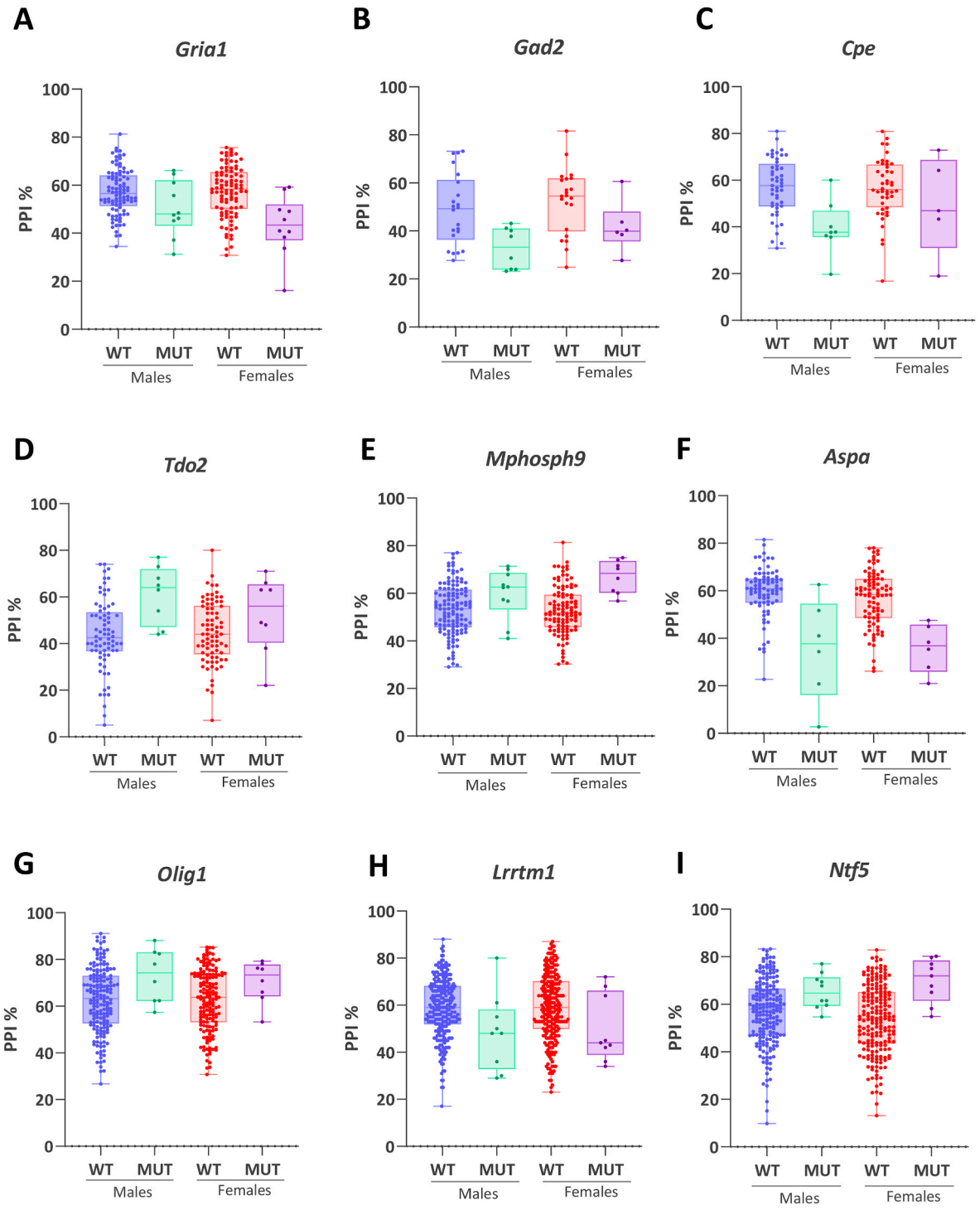

Fig. 2. Prepulse inhibition (PPI) phenotypes associated with disruption of selected mouse genes. (**A**) *Gria1* (Glutamate Ionotropic Receptor AMPA Type Subunit 1), (**B**) *Gad2* (Glutamic acid decarboxylase, 2), (**C**) *Cpe* (Carboxypeptidase E), (**D**) *Tdo2* (Tryptophan 2,3-dioxygenase), (**E**) *Mphosph9* (M-phase phosphoprotein 9), (**F**) *Aspa* (Aspartoacylase), (**G**) *Olig1* (Oligodendrocyte transcription factor 1), (**H**) *Lrrtm1* (Leucine rich repeat transmembrane neuronal 1), (**I**) *Ntf5* (Neurotrophin 5). Comparisons were made using the soft windowing approach of the International Mouse Phenotyping Consortium (IMPC) web resource at www.mousephenotype.org and hence, control group numbers vary accordingly. WT = wildtype control mice, MUT = mutant mice.

expression in the Genotype-Tissue Expression (GTEx) portal. The tissue specificity was tested using the differentially expressed genes (DEGs) as per the description on the FUMA database (https://fuma.ctglab.nl/tutorial#gene2func). The gene symbols were used as the input in each database. Enrichments were considered significant when the Benjamini-Hochberg corrected p value (=q) was less than 0.05.

2.12. Module enrichments for schizophrenia variants and PPI genes

Genome-wide association study (GWAS) summary statistics for Schizophrenia, as identified by the (Schizophrenia Working Group of the Psychiatric GenomicsC, 2014; Trubetskoy et al., 2022), were accessed through the GWAS catalog database (https://www.ebi.ac.uk/gwas/home). The Schizophrenia rare and URVs were those identified by

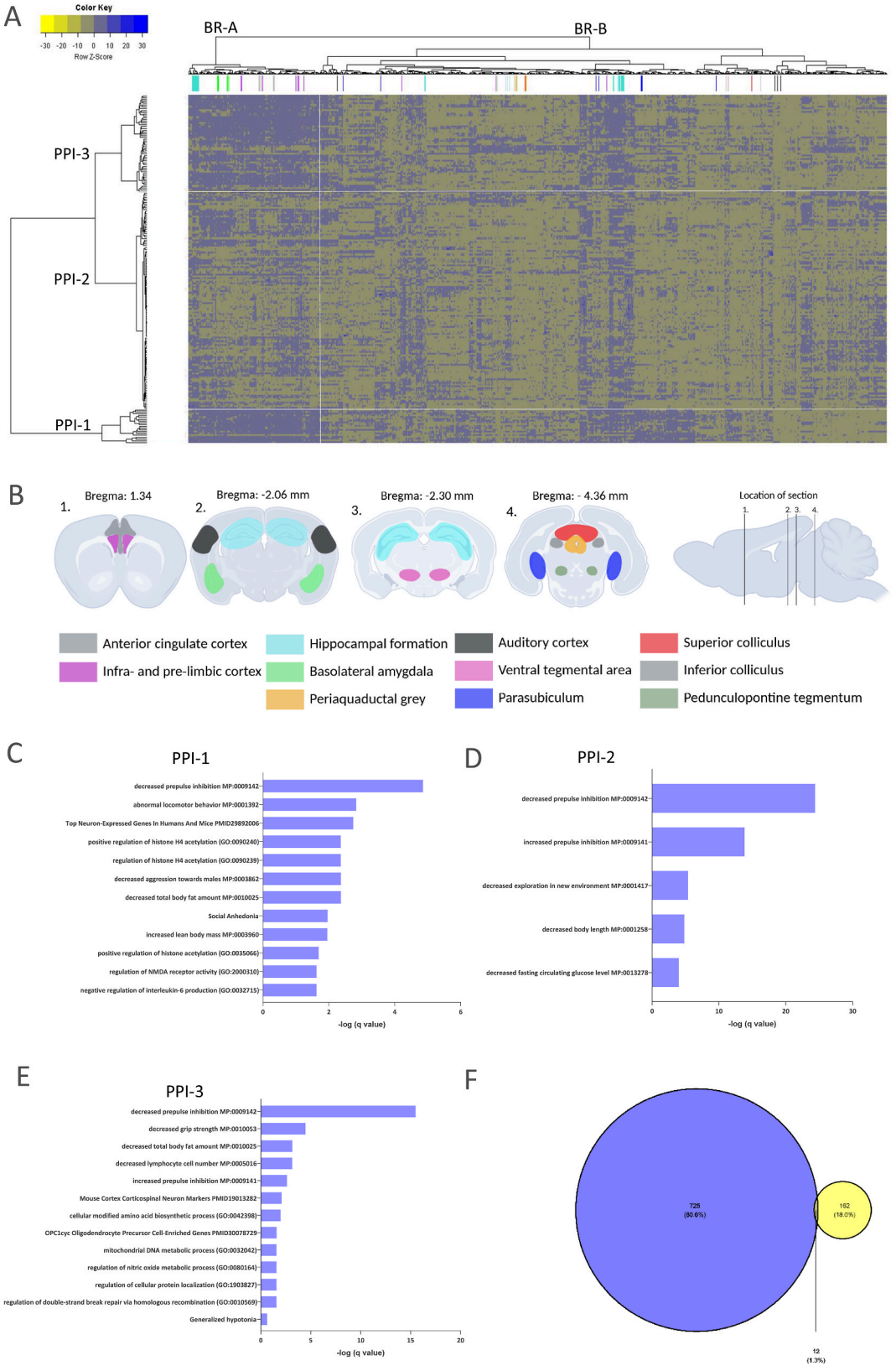

Fig. 3. (**A**) Unsupervised hierarchical clustering analysis of prepulse inhibition (PPI) gene expression in brain. Brain regions (BR) were clustered according to in situ hybridization (ISH) expression values (Allen Brain Atlas) of PPI genes and revealed two clusters (BR-A and BR-B). PPI genes gathered in three clusters PPI-1, PPI-2 and PPI-3. Color-coded lines represent brain regions of interest for PPI. (**B**) Visualization of the color-coded brain regions from the heatmap indicated in mouse brain coronal brain sections with corresponding Bregma levels for each section. Enrichment analyses for each of the PPI gene modules PPI-1 (**C**), PPI-2 (**D**) and PPI-3 (**E**). (**F**) % overlap of PPI genes (188) with Schizophrenia genome wide associated study (GWAS) common variants from GWAS catalog. Created with Biorender. (For interpretation of the references to color in this figure legend, the reader is referred to the Web version of this article.)

(Singh et al., 2022) and consisted of 244 gene variants with unadjusted p value < 0.01. Fisher's exact test was applied to determine whether the number of Schizophrenia variants in a module exceeded the expected number based on the total number of brain-expressed genes and Schizophrenia variants analogous to (Sabik et al., 2021). For the WGCNA, 33 modules (i.e. 17348 genes), including the grey module, were considered in the Fisher's exact test for the calculations of p-values. P-value adjustment was applied using the Benjamini-Hochberg method (Benjamini and Hochberg, 1995). A Fisher's exact test was also used to assess the statistical significance of the PPI gene occurrence in the WGCNA modules.

2.13. Mouse PPI phenotype identification of potential core genes

Using the IMPC database, we performed a batch inquiry of all genes from PPI-1X or the Midnight Blue module. This list was sorted for genes with phenotype information available and the mouse phenotype (MP) term "prepulse inhibition" annotated. The PhenStat package was used to analyse the data for each of the available lines directly. GO, Reactome, KEGG pathway and SynGO enrichment analysis via ENRICHR was conducted to functionally annotate the novel gene list.

2.14. Data availability

Protocols and procedures for all assays are available from mousephenotype.org/impress. Genotype-phenotype associations, detailed statistical results and raw phenotype data are available from mousephenotype.org and can be retrieved from an API or via bulk download as described here: mousephenotype.org/help/data-access/.

3. Results

3.1. Cross-phenotype meta-analysis scores using gene-knockout-to-phenotype association summary statistics

Meta-analysis scores were obtained for each of the 4031 tested genes using four PPI phenotype scores. We excluded thirty-five knockout-lines with a hearing loss phenotype that would preclude PPI testing. For genes tested by multiple centers, a single score was obtained by filtering or pooling. Meta-analysis scores for 198 genes survived a False Discovery Rate threshold of $q \leq 0.06$. 29% of PPI candidate genes were heterozygous deletions while the remainder were homozygous (Supplementary information 1). Furthermore, 80% (~) of these genes were associated with a reduction in PPI in mice, with the remainder associated with increased PPI (Supplementary information 1**, columns P and Q** including www.mousephenotype.org link to data visualization and comparison using the soft windowing analysis (Haselimashhadi et al., 2020)). The graphical visualization of % PPI for a selected subset of these genes is shown in Fig. 2. Overall, these genes have orthologs that represent only a fraction of the human genome. The prioritized genes provide an anchor for the following bioinformatic analysis of mechanisms, neuroanatomical bases, networks and potentially novel core Schizophrenia genes.

3.2. Spatial organization of the PPI gene transcriptome in adult mouse brain

PPI is an established endophenotype for a range of neuropsychiatric disorders including autism spectrum disorders (ASD) and Tourette's syndrome and is not specific to Schizophrenia classifications (Perry et al., 2007; Santos-Carrasco and De la Casa, 2023; Zebardast et al., 2013). Therefore, to identify both the brain regions essential for mediating PPI and the distinct gene expression patterns that will parse the gene set (188 genes with brain expression data in ABA) into functional and disease-coherent modules, we performed a hierarchical clustering analysis based on the organization of the corresponding high-resolution spatial transcriptomic data (ABA, 1707 defined brain areas). We hypothesized that clustering would organize the PPI genes into clusters or modules that share common brain expression patterns and hence broadly similar functions for more robust determination of Schizophrenia relevance.

The cluster analysis gathered the anatomical brain regions into two main clusters (designated BR-A and BR-B Fig. 3A and B, Supplementary information 2). **BR-A** consisted of brain areas derived from embryonic telencephalon including the hippocampus (*dentate gyrus and CA3*), cortex (*anterior cingulate, enthorhinal, parietal, retrosplenial, motor and somatosensory*) and amygdala (*basolateral, lateral*). **BR-B** was composed of a mixture of telencephalic (e.g. *cortical subregions, amygdala nuclei, hippocampal CA1 and CA2, parasubiculum*), diencephalic (e.g. *thalamic and hypothalamic nuclei*), mesencephalic (*ventral tegmental area, brainstem nuclei, inferior colliculus, periaqueductal grey*) and rhombencephalic structures (e.g. *medulla oblongata and pontine nuclei*). Functionally, those regions involved in PPI mediation were gathered only in BR-B while BR-A encompassed only the PPI-modulating brain regions (Rohleder et al., 2016) (Supplementary information 2).

Based on these expression patterns, PPI genes were clustered into 3 modules (designated **PPI-1**, **PPI-2** and **PPI-3,** Supplementary information 3). **PPI-1** gathered 19 genes that were widely expressed but most predominantly in the forebrain PPI-modulating telencephalic regions of BR-A. **PPI-2** consisted of 120 genes with relatively low expression throughout the brain whereas **PPI-3** comprised 54 genes that were also moderately expressed in BR-A. Based on the gene expression profiles of the three PPI gene modules, BR-A is the most clearly distinguishing brain region cluster.

3.3. Three functionally coherent PPI gene modules based on brain expression

We wanted to identify dysregulated mechanisms causing mouse PPI abnormality through the functional coherence of the gene co-expression modules. Enriched terms were deemed significant when the Benjamini-Hochberg corrected p value (=q) was less than 0.05. **PPI-1** genes exhibited high brain-wide expression and are likely fundamental to brain function. They included the glutamatergic neurotransmitter *Gria1* gene (homozygous KO) encoding the GluA1 subunit of α-amino-3-hydroxy-5-methyl-4-isoxazole propionate (AMPA) receptor and the *Gad2* gene (homozygous KO) that encodes the GABAergic synthetic enzyme glutamate decarboxylase 2, both integral to normal brain excitatory and inhibitory activity respectively. Accordingly, enrichment analysis revealed that, collectively, knockout of genes from this module *decreased prepulse inhibition* (as expected) and caused *abnormal locomotor behavior* (*Gria1, Vgf, Ncam2, Cpe*) in mice (Fig. 3C–Supplementary information 4). Furthermore, these genes are among the top neuron-expressed genes in mice and humans (*Gria1, Camk2b, Rtn1, Fus, Gad2, Cpe, Atp6v1c1, Srsf11*) as well as involved in *regulation of NMDA receptor activity* (*Gria1, Camk2b*) and *Social Anhedonia* (*Vgf, Arrb1*). The PPI-1 gene set was highly expressed in the adult brain from late infancy with lower expression during early/mid/late prenatal development indicating a stronger function within the postnatal brain (Supplementary Fig. 1. *GTex, Brainspan*).

The **PPI-2** genes exhibited restricted brain expression, indicating discrete brain region function. Gene deletion altered PPI (both increased and decreased), *decreased exploration of a novel environment*, *decreased body length* and *decreased fasting circulating glucose* (Fig. 3D and Supplementary information 4). There were no clear collective associations of PPI-2 genes with biological processes or disease (GO_Biological Process and DisGeNET, Fig. 3D). Overall, PPI-2 has gathered functionally diverse genes not clearly distinguished when organized based on the brain transcriptome. The lower expression of PPI-2 genes in brain (adult and developing brain) confirms this, with high expression in fallopian tubes, cervix-uterus, lung, breast, nerve and adipose tissue (Supplementary Fig. 1, *GTeX, Brainspan*). *Tdo2* (Tryptophan 2, 3-dioxygenase) is

a gene gathered into this module. The encoded enzyme is highly expressed in the liver with low expression in the brain. It catalyzes the conversion of tryptophan to kynurenine and is associated with Schizophrenia (Miller et al., 2004). Heterozygous knockout of this gene in mice increased PPI in males and females.

Finally, **PPI-3** genes altered PPI (both increased and decreased), as well as decreased grip strength (e.g. *Gatm, Stim2, Prkch, Kdm1a, Aspa*), total body fat (e.g. *Gatm, Stim2, Aspa, Zdhhc5, Sirpa*) and lymphocyte cell number (Fig. 3E–Supplementary information 4). This gene module was also involved in *cellular modified amino acid biosynthetic process* and *mitochondrial DNA metabolic process*. There were no clear disease term associations within this gene set (DisGeNET). Moreover, the PPI-3 gene set was expressed in the adult brain and in the postnatal early infant brain (*GTex, Brainspan* Supplementary Fig. 1) in specific cell populations e.g. cortex corticospinal neuron markers (e.g. *Setd2, Zdhhc5, Stim2, Tmem41b*) and oligodendrocytes (e.g. *Olig1, Gatm,* Fig. 3D, **Supplementary Information 4**).

3.4. Schizophrenia risk and PPI genes converge based on telencephalic expression

To determine whether mouse PPI genes are associated with SZ genetic risk, we assessed the whole PPI gene set and the modules for enrichment of established human common and rare variant genes using the Fisher's exact test (Supplementary information 5). With this approach, we found a significant enrichment (12 overlapping genes) of common (not the rare) variants within the entire PPI gene set indicating convergence of Schizophrenia and PPI genetic risk (Fisher's exact test: $p = 0.039$, Fig. 3F).

Focusing on the individual modules, PPI-1 had the highest proportion of enriched common Schizophrenia variants at **16% (3/19)**, followed by PPI-2 (**6%, 7/120**) and PPI-3 (**4%, 2/52,** see Table 1 and Supplementary information 5). PPI-1 enriched variants included the glutamatergic receptor *Gria1* as well as *Rtn1* (Reticulon 1) and *Camk2b* (Calcium calmodulin-dependent protein kinase IIb) and all three are among the top neuron-expressed genes (Fig. 3C) and ablation decreased PPI (Table 1). *Rtn1* loss also caused abnormal locomotor behavior (altered gait), while *Camk2b* and *Gria1* loss was associated with hyperactivity. The common variants that enriched in PPI-3 were *Zdhhc5* (zinc finger, DHHC domain containing 5) and *Stim2* (stromal interaction molecule 2), both corticospinal-neuron expressed genes (Table 1). Loss of both genes impaired prepulse inhibition and altered the startle reflex (decreased/increased respectively).

3.5. Expanded PPI gene modules based on brain transcriptomic spatial organization

The PPI gene set (188 genes) was identified from the IMPC data (4031 genes) available at the time point of analysis (DR10.1), accounting for only a fraction of the entire protein-coding genome. To address this issue of data incompleteness and create an extended network to enrich established and potentially novel SZ-associated rare variant genes with "core-like" properties, we expanded the gene set by performing a hierarchical clustering analysis of all ABA-available mouse brain transcriptomic data measured by ISH expression. It was our aim to fabricate a more complete co-expression network based on the PPI modulating BR-A telencephalic brain structures that distinguish the PPI gene clusters above (Fig. 3A, PPI-1, -2, -3, (Rohleder et al., 2016).

With the new expanded modules (PPI-1X, PPI-2X, PPI-3X), PPI-1X gathered 2058 genes that included all but one (*Gad2*) of the original PPI-1 genes while PPI-2X comprised 15579 genes that included all but three of the original PPI-2 genes and PPI-3X gathered 3897 genes that included all except 14 of the original PPI-3 genes (Fig. 4A, Supplementary information 6). We hypothesized that the new expanded gene modules (i.e. the gene clusters PPI-1X, PPI-2X, PPI-3X) resemble the original ones (PPI-1, PPI-2, PPI-3) based on similar expression profiles within each module and because most genes from the original modules are included in the expanded modules.

3.6. Mouse PPI-1X identified as schizophrenia-relevant core gene module

To determine whether genes in the expanded gene modules harbor genetic risk for Schizophrenia, we investigated enrichment of common variant mutations with Fisher's exact test and manual annotation of ultra-rare variants (URVs). Regarding the overlap of the URV genes (Singh et al., 2022), the highest proportion was found in **PPI-1X** (2.6%), the module with highest expression across brain regions (Supplementary information 7). Based on this pattern, we therefore designated PPI-1X as the "core" module for identification of rare Schizophrenia variant genes. The greatest proportion of overlapping common variant genes occurred in **PPI-3X** followed by PPI-1X (Schizophrenia Working Group of the Psychiatric GenomicsC, 2014; Trubetskoy et al., 2022). The smallest proportion but the most significant enrichment occurred in PPI-2X owing to the larger sample size (Supplementary information 8) (PPI-1X: 116 overlapping genes, 4.7%, Fisher's $P\ adj = 2.38^{e-08}$, PPI-2X: 431 overlapping genes, 2.9%, Fisher's $P\ adj = 5.66^{e-21}$, PPI-3X: 229 overlapping genes, 5.4%, Fisher's $P\ adj = 1.85^{e-16}$, Fig. 4B).

As well as the expected Schizophrenia disease annotation of the overlapping common variant genes, there were additional disease comorbidity associations (Fig. 4C–H, Supplementary information 9). The rare and common variants that enriched within PPI-1X were also associated with, for example, intellectual disability, epilepsy/seizures and severe mental retardation. PPI-1X, PPI-2X and PPI-3X common variants were also associated with ASDs. Regarding functional profiles, PPI-1X rare and common schizophrenia variant genes were associated with the mammalian phenotype *hyperactivity*, abnormal synaptic transmission, *abnormal long-term spatial reference memory,* and *reduced long-term potentiation* (Fig. 4C–H, Supplementary information 9, columns A-F and H-M). The profile for PPI-3X overlapping Schizophrenia common variant genes included the mammalian phenotypes of *impaired*

Table 1
Schizophrenia common variants enriched in the prepulse inhibition clusters.

Mouse Gene	Protein	Annotation	Mouse knockout	Sex	PPI phenotype	PPI cluster
Rtn1	RTN1	Reticulon-1	−/−	M, F	decreased	1
Gria1	GRIA1	Glutamate receptor 1	−/−	M, F	decreased	1
Camk2b	CAMK2B	Calcium/calmodulin-dependent protein kinase type II subunit beta	+/−	F	decreased	1
Mgmt	MGMT	Methylated-DNA–protein-cysteine methyltransferase	−/−	M, F	decreased	2
Bach 2	BACH2	BTB and CNC homology, basic leucine zipper transcription factor 2	−/−	M, F	decreased	2
Tfr2	TFR2	Transferrin receptor protein 2	−/−	M, F	decreased	2
Nhlh1	NHLH1	Helix-loop-helix protein 1	+/−	F	decreased	2
Ghrhr	GHRHR	Growth hormone-releasing hormone receptor	−/−	M, F	decreased	2
Efcab6	EFCAB6	EF-hand calcium-binding domain-containing protein 6	−/−	M, F	decreased	2
Mphosph9	MPHOSPH9	M-phase phosphoprotein 9	−/−	M, F	increased	3
Zdhhc5	ZDHHC5	Palmitoyltransferase ZDHHC5	−/−	M, F	decreased	3
Stim2	STIM2	Stromal interaction molecule 2	+/−	M, F	decreased	3

M = male, F = females.

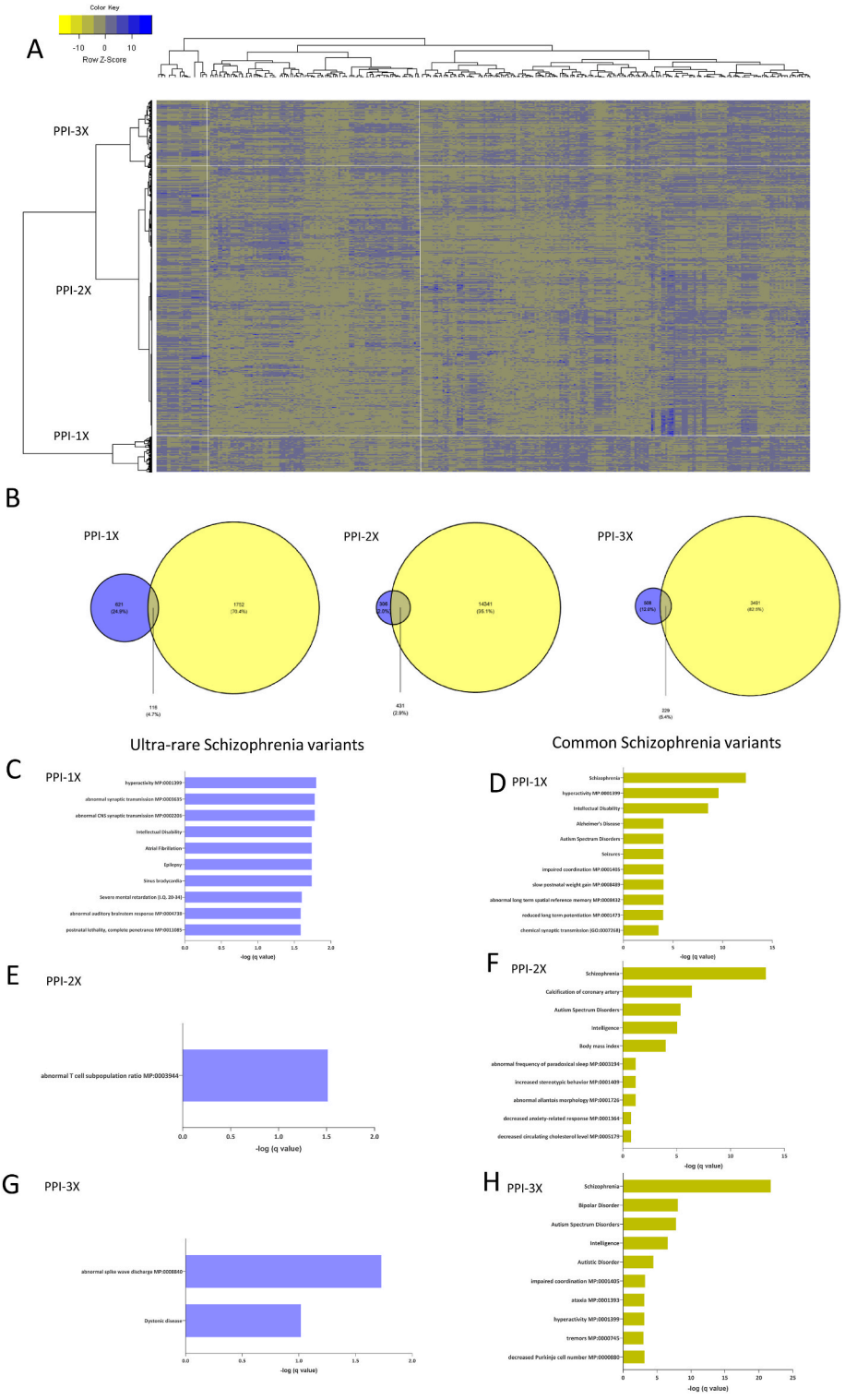

Fig. 4. (**A**) Unsupervised hierarchical clustering of transcriptomic data from entire genome based on BR-A. Brain regions (BR) were clustered according to in situ hybridization (ISH) expression values (Allen Brain Atlas) and revealed three brain region clusters. Genes gathered in three extended clusters (I, II, III). **(B)** The overlap of established schizophrenia common variants with each of the extended clusters. **(C, D, E)**. Enrichment analyses for each of the Schizophrenia ultra-rare and common variant gene overlaps with each of the extended gene modules are shown.

coordination and *decreased Purkinje cell number*.

3.7. Human Midnight Blue identified as schizophrenia core gene module

We applied an alternative human brain-based method to elucidate Schizophrenia core gene modules using those from an established WGCNA of resting-state healthy human donor tissue in ABA (Hawrylycz et al., 2015). The WGCNA is a correlation network approach that determines gene-to-gene associations by grouping similarly expressed genes together for functional annotation and unearthing novel genes. In the assessment of 33 co-expression modules, we observed that the common GWAS variants were significantly (with $q < 0.05$) enriched in 5

modules (Modules M1 (Midnight Blue), M2 (Saddle Brown), M4 (White), M6 (Pink) and M11 (Brown)) (Fig. 5A, Supplementary information 10) and the URVs in one module (M1 (Midnight Blue), Fig. 5A–Supplementary information 11). The PPI genes did not enrich significantly (with q < 0.05) in any modules however, there were nominally significant enrichments in two modules (M11 (Brown), M12 (Antique White)) with an unadjusted p-value (Fig. 5A–Supplementary information 12). Module M1 ("**Midnight Blue**") enriched both the common and rare variants, and tended to enrich for PPI genes, and we, therefore, designated this as the Schizophrenia core gene module from this analysis (**Supplementary information 10, 11, 12**).

Midnight Blue consists of 451 genes assigned to Telencephalon. This encompassed parts of the frontal, parietal and temporal lobes, cingulate gyrus and caudate putamen. The highest expression of these genes was in hippocampus, particularly the dentate gyrus, and the amygdala including basolateral amygdala. With parallels to PPI-1X, this module was associated with synaptic transmission and regulation of synaptic plasticity (Hawrylycz et al., 2015). Hyperactivity, enhanced long-term potentiation, and decreased anxiety-related response phenotypes associated with these genes (Fig. 5B). That the Schizophrenia risk gene sets significantly, and the PPI genes tend to, enrich within this module is consistent with findings from our mouse brain tissue co-expression hierarchical clustering. The BR-A brain region cluster from this analysis was restricted to forebrain Telencephalic structures that included those involved in PPI modulation (Rohleder et al., 2016).

3.8. Using mouse PPI to identify novel schizophrenia genes in human and mouse core co-expression modules

We wanted to identify novel "core" Schizophrenia-relevant PPI genes based on similar neuroanatomical patterning and the "guilt-by-association" rule. With two independent methods in mice and humans, we identified PPI-1X (from clustering) and Midnight Blue (from WGCNA) as "core modules". 50% of Midnight Blue enriched-URV genes overlapped with PPI-1X (Singh et al., 2022). Using IMPC PhenStat and batch queries, we determined that 7% of available PPI-1X- and Midnight Blue gene-KO mouse models exhibit robust PPI phenotypes (p < 0.0001, **Supplementary information 13, 14**). From this gene subset, we excluded established URVs and common variants and genes from the original DR10.1 PPI list and focused on the newly generated DR19.1 (October 2023) PPI additions. The remaining PPI genes from both core modules were designated "potentially novel" core genes with PPI endophenotypes (full list in **Supplementary Information 15**) and listed in Tables 2 and 3 (details in **Supplementary Information 15**).

Established Schizophrenia-related PPI genes detected by both methods were the previously described *Gria1* and *Camk2b*. Looking at both sets of novel PPI genes (from PPI-1X and Midnight Blue) together, a subnetwork of genes was associated with *abnormal auditory brainstem response* and *decreased startle reflex* indicating hearing abnormalities that would preclude clear detection of PPI impairments (*Nin, Aak1, Nedd4l, Ckb, Dyrk1b,* and *Nptn* KO mice). Thus, we excluded these genes from the final list of "novel" PPI genes.

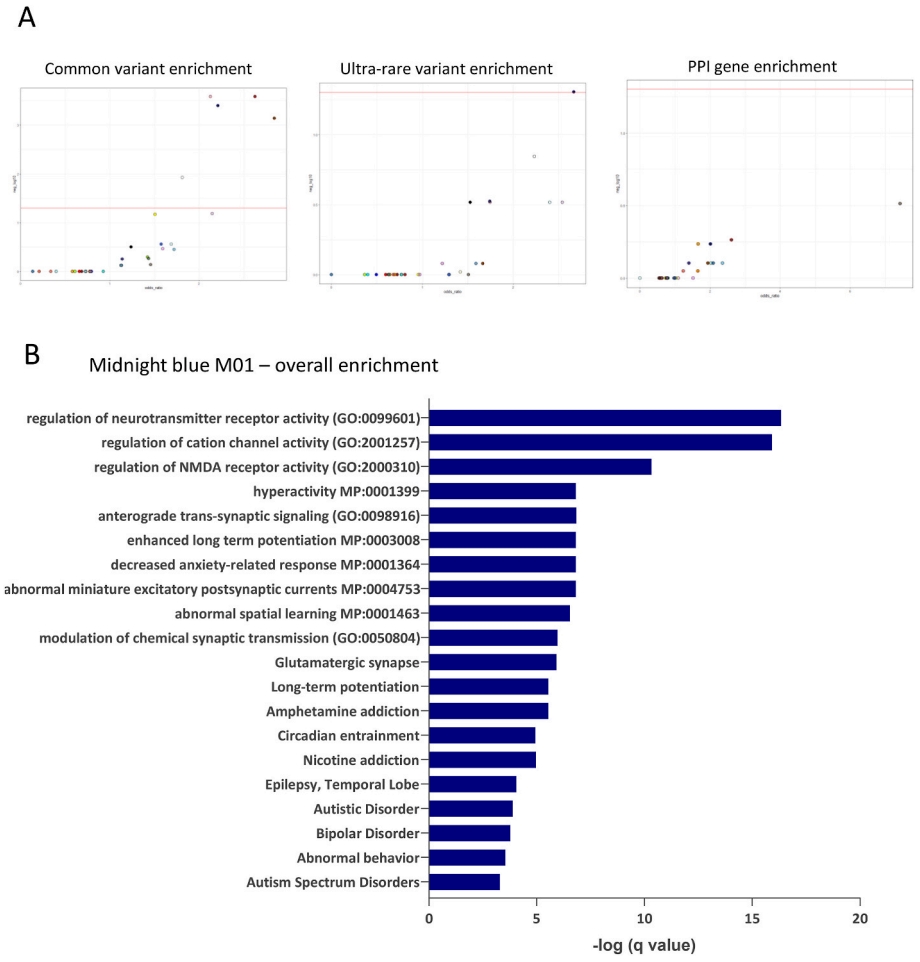

Fig. 5. Schizophrenia-relevant „core" genes enriched in Midnight Blue module. **(A)** Module enrichments for established Schizophrenia common and rare variants and mouse prepulse inhibition (PPI) genes. The Midnight Blue module is significantly enriched in common and ultra-rare variants and tends to be enriched in mouse PPI genes. The red line in each plot indicates the significance threshold of padj <0.05. **(B)** Midnight Blue module functional and disease annotations. (For interpretation of the references to color in this figure legend, the reader is referred to the Web version of this article.)

Table 2
PPI-1X novel PPI genes with Schizophrenia core-like properties.

Mouse symbol	Human gene	Gene name
Ctsa	*CTSA*	Cathepsin A
Sbf1	*SBF1*	SET binding factor 1
Tspyl2	*TSPYL2*	TSPY-like 2
Tanc2	***TANC2***	**Tetratricopeptide repeat, ankyrin repeat and coiled-coil containing 2**
Arih1	*ARIH1*	Ariadne RBR E3 ubiquitin protein ligase 1
Tpm 1	*TPM1*	Tropomyosin alpha-1 chain
Tspan13	*TSPAN13*	Tetraspanin-13
Aven	*AVEN*	Apoptosis And Caspase Activation Inhibitor
Cs	*CS*	Citrate synthase
Marchf6	*MARCHF6*	Membrane associated ring–CH–type finger 6
Ntrk2	*NTRK2*	BDNF/NT-3 growth factors receptor
Pak1	*PAK1*	P21 (RAC1) Activated Kinase 1
Snrnp70	*SNRNP70*	Small Nuclear Ribonucleoprotein U1 Subunit 70
Clk 2	*CLK2*	CDC Like Kinase 2
Mib2	*MIB2*	MIB E3 Ubiquitin Protein Ligase 2
Rgl1	*RGL1*	Ral guanine nucleotide dissociation stimulator-like 1
Gpcpd1	*GPCPD1*	Glycerophosphocholine Phosphodiesterase 1
Snx14	*SNX14*	Sorting nexin-14
Mpi	*MPI*	Mannose-6-phosphate isomerase
Mat2a	*MAT2A*	methionine adenosyltransferase 2A
Spock 1	*SPOCK1*	SPARC (Osteonectin), Cwcv And Kazal Like Domains Proteoglycan 1
Tspoap1	*TSPOAP1*	TSPO associated protein 1
Atp5f1b	*ATP5F1B*	ATP Synthase F1 Subunit Beta
Fkbp10	*FKBP10*	FKBP Prolyl Isomerase 10
Tlcd3b	*TLCD3B*	TLC Domain Containing 3B

Table 3
WGCNA Midnight Blue novel PPI with Schizophrenia core-like properties.

Mouse symbol	Human gene	Gene name
Frrs1l	*FRRS1L*	Ferric-chelate reductase 1 like
Ccsap	*CCSAP*	Centriole, cilia and spindle associated protein
Brd 4	*BRD4*	Bromodomain-containing Protein 4
Abi2	*ABI2*	Abl interactor 2
Tanc2	***TANC2***	**Tetratricopeptide repeat, ankyrin repeat and coiled-coil containing 2**
Camk1	*CAMK1*	Calcium/calmodulin dependent protein kinase I

Among the novel PPI genes, the other predominant mouse phenotype was hyperactivity (*Abi2, Tspyl2, Frrs1l, Ntrk2, Arih1,* and *Ccsap* KO mice). SynGO analysis also indicates that there was a preponderance of synaptic genes particularly representing the postsynapse (TANC2, PAK1, ABI2, CAMK2, NTRK2, **Supplementary Information 16**). A novel core gene identified in both the PPI-1X and Midnight Blue modules was *TANC2*. Tetratricopeptide repeat, ankyrin repeat and coiled-coil containing 2 (TANC2) is a post-synaptic scaffold protein associated with neurodevelopment, intellectual disability and autistic features (Garrett et al., 2022; Guo et al., 2019). Based on GO and Reactome analysis of the novel PPI genes (**Supplementary information 15**), TANC2 was part of a subnetwork with other genes implicated in brain development including regulation of axonogenesis (NTRK2, PAK1), regulation of neuron projection development (PAK1, NTRK2, CAMK1, SPOCK1, ABI2, TANC2) and NOTCH signaling (MIB2). There were also genes involved in oxidative phosphorylation, the citrate cycle, glyoxylate and dicarboxylate metabolism (CS, ATP5F1B) and chaperone-mediated autophagy (CTSA, SNRNP70). Genes from specific brain cell populations also emerged including CTSA (in microglia), MAT2A (in astrocytes) and PAK1 (in oligodendrocytes).

4. Discussion

Schizophrenia has a complex polygenic architecture consisting of both common and rare variants in hundreds of candidate genes (Singh et al., 2022; Trubetskoy et al., 2022). Nevertheless, this established genetic risk has yet to transduce into mechanisms of phenotypic heterogeneity, improved treatment strategies and patient stratification. We used IMPC mouse PPI data with mesoscale neuroanatomic analysis to functionally interrogate and prioritize Schizophrenia variants employing computational analysis through the Omnigenic hypothesis. To this end, we took a cross-species approach integrating mouse PPI genes with mouse (hierarchical clustering) and human (WGCNA) brain spatial gene expression data. We determined that the genetic substrates of mouse PPI significantly align with human Schizophrenia risk genes. Furthermore, based on brain expression, we identified PPI- and Schizophrenia-relevant functionally coherent modules with established and potentially novel "core-like" genes involved in neurotransmission/synaptic function. These genes will be important for informing Schizophrenia-related rare genes and druggable target elucidation.

Human disease gene discovery remains correlative with existing methods (Claussnitzer et al., 2020) and macroscopic MRI does not reveal molecular and cellular abnormality (Keshavan et al., 2020). Integrating KO mouse PPI with brain expression data therefore provides a powerful platform to translate human genetic risk into Schizophrenia-relevant brain pathology. We found a significant convergence of Schizophrenia and mouse PPI risk genes through both co-expression analyses. Thus, in concordance with previous analysis (Zeighami et al., 2023), rodent models sufficiently represent this aspect of human Schizophrenia molecular pathology, not thwarted by inter-species biological and gene homology differences (Monaco et al., 2015). Combined, this supports the utility of meticulously controlled data generated from multiple mouse models to understand human Schizophrenia genetic risk neurobiology.

PPI abnormality is not specific to Schizophrenia and has transdiagnostic potential (Insel et al., 2010; Santos-Carrasco and De la Casa, 2023). Thus, we wanted to find a specific PPI-gene subnetwork with Schizophrenia core-like properties (Boyle et al., 2017). Telencephalic PPI modulating brain regions emerged as the most relevant for the PPI/Schizophrenia overlap, consistent with strong telencephalic transcriptional patterning of psychiatric disorders (Zeighami et al., 2023). Three established neuro-circuits underlie the PPI response: startle mediating, PPI mediating and PPI modulating. Broadly, PPI mediation recruits mid/hind brain regions while PPI modulation, on the other hand, implicates the cortex including anterior cingulate, hippocampus and amygdala among others (Rohleder et al., 2016). The anterior cingulate is part of the human dorsolateral prefrontal cortex controlling executive function. This region, along with the hippocampus, frequently malfunctions in Schizophrenic patients (Huckins et al., 2019; Yoon et al., 2008). It was the synaptic/neurotransmission genes with highest expression in the PPI modulating regions (PPI-1X and Midnight Blue) that strongly associated with Schizophrenia risk. This combined pattern is consistent with existing glutamate and dendritic pathology Schizophrenia hypotheses, further confirming altered glutamatergic and synaptic plasticity as the cornerstone of the disease pathogenesis (Coyle, 2012; Fromer et al., 2014). With this confirmation, we thus provide a framework for attributing Schizophrenia disease coherence to mouse PPI genes and for functionally annotating existing and undisclosed Schizophrenia variant genes.

With two established core modules, we identified a litany of potentially novel Schizophrenia "core-like" genes. The Omnigenic model proclaims that all genes expressed in a disease-relevant tissue contribute to variation, but it is the core genes that directly influence the trait, in this case, PPI (Boyle et al., 2017). By this definition, TANC2 emerged from both approaches. Expressed in the developing and adult brain in the postsynaptic density scaffold, homozygous deletion impaired PPI and caused hyperactivity (Garrett et al., 2022). Although evidence is limited, there are hints supporting a Schizophrenia role for TANC2. This includes a *de novo* missense TANC2 variant (p.794A > V) in a female Schizophrenic patient (Fromer et al., 2014) and how machine learning

differentiated Schizophrenia from bipolar and major depressive disorder based on TANC2 (Yang et al., 2022). Moreover, this gene exemplifies how allelic heterogeneity varies symptom severity depending on the mutation. To date (Guo et al., 2019), only monoallelic patient mutations are described whereas biallelic deletion underlies the mouse PPI phenotype. This is consonant with the gradient effect of neurodevelopmental mutations where high disruption is more strongly associated with intellectual disability than SZ (Fromer et al., 2014). Thus, more evidence is required to determine whether the developmental or adult-derived function of TANC2 potentially increases Schizophrenia genetic risk. Other developmental genes did however emerge as "core" genes (e.g. *PAK1, SPOCK1*) supporting the Schizophrenia neurodevelopmental hypothesis (Fatemi and Folsom, 2009). In addition, the novel core genes emblematic of diverse functional and biological categories, including brain bioenergetics and glial cells (oligodendrocytes, microglia and astrocytes), are consistent with Schizophrenia complexity for which this computational framework can be applied for annotation (Brown et al., 2021).

A salient issue influencing PPI diagnostic value concerns the alignment with positive and negative Schizophrenia symptoms. At least in male patients, PPI correlates with both symptom domains (Braff et al., 1999). We observed a similar pattern in this study, however there was a functional dichotomy depending on the co-expression module involved. The PPI-1 (and PPI-1X) module of synaptic brain-wide expressed PPI genes was phenotypically associated with mouse hyperactivity. The latter is a putative proxy for psychomotor agitation, a positive symptom aligning with delusions and impaired self-control (Pompili et al., 2021). The PPI-3 (and PPI-3X) genes on the other hand associated with impaired grip, hypotonia, corticospinal motor output neurons (CSNs, from motor M1 and somatosensory S1 cortex) and myelin-producing oligodendrocytes (Baumann and Pham-Dinh, 2001; Macias et al., 2022). That abnormal motor control is a Schizophrenia negative symptom could indicate that common variant genes that predominate in PPI-3 are relevant for this symptom domain (Abboud et al., 2017). Different NPD co-morbidities were also evident within this functional dichotomy such as Intellectual Disability with brain-wide expressed neuronal function genes (PPI-1X) and ASD with expression in specific cell populations (PPI-3X). This indicates risk for cognitive impairment with PPI-1X gene loss-of-function-mutations (Fromer et al., 2014). Moreover, as in the example of TANC2, while overlapping genes are involved in Schizophrenia and other neurodevelopmental disorders, the severity of functional effects depends on the mutation. Thus, focusing on PPI molecular underpinnings has the potential to reduce heterogeneity and reveal novel clinical strata and transdiagnostics for the RDoC (Insel et al., 2010; Owen, Legge, Rees, Walters and O'Donovan, 2023; Santos-Carrasco and De la Casa, 2023). Future dissection of how rare and common variants fall within this functional dichotomy will be important for patient stratification and developing treatment strategies for negative symptoms.

We based this analysis on the Omnigenic model as a broad theoretical construct and tool to estimate the likely proximity of PPI genes to Schizophrenia pathogenesis based on co-expression analysis. Nevertheless, this theory has been debated and criticized previously for a disproportionate focus on "core" genes and an over-simplification of the definition of core vs. peripheral genes (Boyle et al., 2017; Wray et al., 2018). These caveats should therefore be borne in mind when considering the results of this study, acknowledging that further empirical analysis is needed to confirm the association of the novel genes with Schizophrenia pathogenesis. Studies such as this one integrating phenomic (in this case, mouse) data with gene co-expression networks, will, in any case, help to evolve and nuance this theory and gene categorization further, increasing the utility for understanding complex neuropsychiatric disease genetic risk.

4.1. Conclusion

In conclusion, we have demonstrated how using mice to understand the genetic substrates and risk in PPI can generate valuable information potentially for better diagnosing and treating Schizophrenia patients. We also provide a neuroanatomic transcriptomic-patterning model derived from mouse PPI modulation to functionally characterize novel disease variants, stratify patients for improved precision treatment approaches, and disclose the genetic underpinnings of phenotypic heterogeneity in Schizophrenia. As PPI is a transdiagnostic endophenotype within the RDoC initiative, a similar cross-disorder analysis could be applied to ascertain the relevance of this mouse phenotype. Furthermore, as most NPD-relevant genetic variation occurs in non-coding regulatory regions (Rummel et al., 2023), future analysis will incorporate regulatory network information to understand the impact on PPI protein-coding gene function (van Dam et al., 2018). In addition, as genes operate in networks or pathways, a systems-level analysis of the core PPI genes identified here will earmark Omnigenic model-relevant peripheral genes through interaction networks.

Funding

This study was funded in parts by the German Federal Ministry of Education and Research (Infrafrontier grant 01KX1012 to MHdA), the German Center for Diabetes Research (DZD) (MHdA) and the Bavarian State Ministry of Science and the Arts (Staatsministerium für Wissenschaft und Kunst) within the initial phase of the German Center for Mental Health (Deutsches Zentrum für Psychische Gesundheit [DZPG] (grant: 01EE2303E).

Competing interests

The authors declare no competing interests.

IMPC consortium

Juan A. Aguilar-Pimental, Oana V. Amarie, Lore Becker, Julia Calzada-Wack, Patricia Da Silva-Buttkus, Nathalia Dragano, Markus Kraiger, Christoph Lengger, Stefanie Leuchtenberger, Susan Marschall, Manuela A. Oestereicher, Birgit Rathkolb, Adrián Sanz-Moreno, Claudia Seisenberger, Nadine Spielmann, Claudia Stoeger, Vivek Kumar, Piia Keskivali, Ruairidh King, Hamed Haselimashhadi, Alexandr Bezginov, Clare Norris, Sarah Taylor, Dale Pimm, Lois Kelsey, Zorana Berberovic, Dawei Qu, Abigail D'Souza, Vivian Bradaschia, Mohammed Eskandarian, Xueyuan Shang, Kyle Duffin, Kyle Roberton, Catherine Xu, Gloria Baguinat, Valerie Laurin, Qing Lan, Gillian Sleep, Lauri Lintott, Marina Gertsenstein, Sandra Tondat, Maribelle Cruz, David Miller, Alexandr Bezginov, Tania Sorg, Fabrice Riet, Heather Tolentino, Todd Tolentino, Mike Schuchbauer, Nichole Hockenbury, Karrie Beeman, Sheryl Pedroia, Jason Salazar, Mollie Heffner, Joanne Hsu, Colin Fletcher, Maya Vanzanten, Elisabetta Golini, John R Seavitt, Denise G Lanza, Isabel Lorenzo, Angelina Gaspero, Amanda Rios.

Acknowledgements

The authors would like to thank all laboratory staff members and animal technicians at IMPC phenotyping centers for their excellent technical skills and dedication. This work would not have been possible without support of the IMPC phenotyping centers by NIH grants U42 OD011175 and UM1 OD023221 (KOMP2) (to KCKL and CM), UM1HG006348 (to MED and JDH), Genome Canada and Ontario Genomics grant OGI-051 (to CM), the French Agence Nationale de la Recherche grants ANR-10-IDEX-0002-02, ANR-10-LABX-0030-INRT, ANR-10-INBS-07 PHENOMIN (YH).

Appendix A. Supplementary data

Supplementary data to this article can be found online at https://doi.org/10.1016/j.nsa.2024.104075.

References

Abboud, R., Noronha, C., Diwadkar, V.A., 2017. Motor system dysfunction in the schizophrenia diathesis: neural systems to neurotransmitters. Eur. Psychiatr. 44, 125–133. https://doi.org/10.1016/j.eurpsy.2017.04.004.

Baumann, N., Pham-Dinh, D., 2001. Biology of oligodendrocyte and myelin in the mammalian central nervous system. Physiol. Rev. 81 (2), 871–927. https://doi.org/10.1152/physrev.2001.81.2.871.

Benjamini, Y., Hochberg, Y., 1995. Controlling the false discovery rate: a practical and powerful approach to multiple testing. J. Roy. Stat. Soc. B 57 (1), 289–300.

Boyle, E.A., Li, Y.I., Pritchard, J.K., 2017. An expanded View of complex traits: from polygenic to omnigenic. Cell 169 (7), 1177–1186. https://doi.org/10.1016/j.cell.2017.05.038.

Braff, D.L., Swerdlow, N.R., Geyer, M.A., 1999. Symptom correlates of prepulse inhibition deficits in male schizophrenic patients. Am. J. Psychiatr. 156 (4), 596–602. https://doi.org/10.1176/ajp.156.4.596.

Brown, S.D., Moore, M.W., 2012. Towards an encyclopaedia of mammalian gene function: the International Mouse Phenotyping Consortium. Dis Model Mech 5 (3), 289–292. https://doi.org/10.1242/dmm.009878.

Brown, T.L., Hashimoto, H., Finseth, L.T., Wood, T.L., Macklin, W.B., 2021. PAK1 positively regulates oligodendrocyte morphology and myelination. J. Neurosci. 41 (9), 1864–1877. https://doi.org/10.1523/JNEUROSCI.0229-20.2021.

Cannon, T.D., Keller, M.C., 2006. Endophenotypes in the genetic analyses of mental disorders. Annu. Rev. Clin. Psychol. 2, 267–290. https://doi.org/10.1146/annurev.clinpsy.2.022305.095232.

Chen, E.Y., Tan, C.M., Kou, Y., Duan, Q., Wang, Z., Meirelles, G.V., Ma'ayan, A., 2013. Enrichr: interactive and collaborative HTML5 gene list enrichment analysis tool. BMC Bioinf. 14, 128. https://doi.org/10.1186/1471-2105-14-128.

Claussnitzer, M., Cho, J.H., Collins, R., Cox, N.J., Dermitzakis, E.T., Hurles, M.E., McCarthy, M.I., 2020. A brief history of human disease genetics. Nature 577 (7789), 179–189. https://doi.org/10.1038/s41586-019-1879-7.

Correll, C.U., Schooler, N.R., 2020. Negative symptoms in schizophrenia: a review and clinical guide for recognition, assessment, and treatment. Neuropsychiatric Dis. Treat. 16, 519–534. https://doi.org/10.2147/NDT.S225643.

Coyle, J.T., 2012. NMDA receptor and schizophrenia: a brief history. Schizophr. Bull. 38 (5), 920–926. https://doi.org/10.1093/schbul/sbs076.

Fatemi, S.H., Folsom, T.D., 2009. The neurodevelopmental hypothesis of schizophrenia, revisited. Schizophr. Bull. 35 (3), 528–548. https://doi.org/10.1093/schbul/sbn187.

Fromer, M., Pocklington, A.J., Kavanagh, D.H., Williams, H.J., Dwyer, S., Gormley, P., O'Donovan, M.C., 2014. De novo mutations in schizophrenia implicate synaptic networks. Nature 506 (7487), 179–184. https://doi.org/10.1038/nature12929.

Garrett, L., Da Silva-Buttkus, P., Rathkolb, B., Gerlini, R., Becker, L., Sanz-Moreno, A., Hrabe de Angelis, M., 2022. Post-synaptic scaffold protein TANC2 in psychiatric and somatic disease risk. Dis Model Mech 15 (3). https://doi.org/10.1242/dmm.049205.

Garrett, L., Trumbach, D., Spielmann, N., Wurst, W., Fuchs, H., Gailus-Durner, V., Holter, S.M., 2023. A rationale for considering heart/brain axis control in neuropsychiatric disease. Mamm. Genome 34 (2), 331–350. https://doi.org/10.1007/s00335-022-09974-9.

Guo, H., Bettella, E., Marcogliese, P.C., Zhao, R., Andrews, J.C., Nowakowski, T.J., Eichler, E.E., 2019. Disruptive mutations in TANC2 define a neurodevelopmental syndrome associated with psychiatric disorders. Nat. Commun. 10 (1), 4679. https://doi.org/10.1038/s41467-019-12435-8.

Haselimashhadi, H., Mason, J.C., Munoz-Fuentes, V., Lopez-Gomez, F., Babalola, K., Acar, E.F., Meehan, T.F., 2020. Soft windowing application to improve analysis of high-throughput phenotyping data. Bioinformatics 36 (5), 1492–1500. https://doi.org/10.1093/bioinformatics/btz744.

Hawrylycz, M., Miller, J.A., Menon, V., Feng, D., Dolbeare, T., Guillozet-Bongaarts, A.L., Lein, E., 2015. Canonical genetic signatures of the adult human brain. Nat. Neurosci. 18 (12), 1832–1844. https://doi.org/10.1038/nn.4171.

Huckins, L.M., Dobbyn, A., Ruderfer, D.M., Hoffman, G., Wang, W., Pardinas, A.F., Stahl, E.A., 2019. Gene expression imputation across multiple brain regions provides insights into schizophrenia risk. Nat. Genet. 51 (4), 659–674. https://doi.org/10.1038/s41588-019-0364-4.

Insel, T., Cuthbert, B., Garvey, M., Heinssen, R., Pine, D.S., Quinn, K., Wang, P., 2010. Research domain criteria (RDoC): toward a new classification framework for research on mental disorders. Am. J. Psychiatr. 167 (7), 748–751. https://doi.org/10.1176/appi.ajp.2010.09091379.

Keshavan, M.S., Collin, G., Guimond, S., Kelly, S., Prasad, K.M., Lizano, P., 2020. Neuroimaging in schizophrenia. Neuroimaging Clin. 30 (1), 73–83. https://doi.org/10.1016/j.nic.2019.09.007.

Kuleshov, M.V., Jones, M.R., Rouillard, A.D., Fernandez, N.F., Duan, Q., Wang, Z., Ma'ayan, A., 2016. Enrichr: a comprehensive gene set enrichment analysis web server 2016 update. Nucleic Acids Res. 44 (W1), W90–W97. https://doi.org/10.1093/nar/gkw377.

Lein, E.S., Hawrylycz, M.J., Ao, N., Ayres, M., Bensinger, A., Bernard, A., Jones, A.R., 2007. Genome-wide atlas of gene expression in the adult mouse brain. Nature 445 (7124), 168–176. https://doi.org/10.1038/nature05453.

Loh, P.R., Bhatia, G., Gusev, A., Finucane, H.K., Bulik-Sullivan, B.K., Pollack, S.J., Price, A.L., 2015. Contrasting genetic architectures of schizophrenia and other complex diseases using fast variance-components analysis. Nat. Genet. 47 (12), 1385–1392. https://doi.org/10.1038/ng.3431.

Macias, M., Lopez-Virgen, V., Olivares-Moreno, R., Rojas-Piloni, G., 2022. Corticospinal neurons from motor and somatosensory cortices exhibit different temporal activity dynamics during motor learning. Front. Hum. Neurosci. 16, 1043501 https://doi.org/10.3389/fnhum.2022.1043501.

Marshall, C.R., Howrigan, D.P., Merico, D., Thiruvahindrapuram, B., Wu, W., Greer, D.S., Schizophrenia Working Groups of the Psychiatric Genomics, C, 2017. Contribution of copy number variants to schizophrenia from a genome-wide study of 41,321 subjects. Nat. Genet. 49 (1), 27–35. https://doi.org/10.1038/ng.3725.

Mena, A., Ruiz-Salas, J.C., Puentes, A., Dorado, I., Ruiz-Veguilla, M., De la Casa, L.G., 2016. Reduced prepulse inhibition as a biomarker of schizophrenia. Front. Behav. Neurosci. 10, 202. https://doi.org/10.3389/fnbeh.2016.00202.

Miller, C.L., Llenos, I.C., Dulay, J.R., Barillo, M.M., Yolken, R.H., Weis, S., 2004. Expression of the kynurenine pathway enzyme tryptophan 2,3-dioxygenase is increased in the frontal cortex of individuals with schizophrenia. Neurobiol. Dis. 15 (3), 618–629. https://doi.org/10.1016/j.nbd.2003.12.015.

Monaco, G., van Dam, S., Casal Novo Ribeiro, J.L., Larbi, A., de Magalhaes, J.P., 2015. A comparison of human and mouse gene co-expression networks reveals conservation and divergence at the tissue, pathway and disease levels. BMC Evol. Biol. 15, 259. https://doi.org/10.1186/s12862-015-0534-7.

Owen, M.J., Legge, S.E., Rees, E., Walters, J.T.R., O'Donovan, M.C., 2023. Genomic findings in schizophrenia and their implications. Mol. Psychiatr. https://doi.org/10.1038/s41380-023-02293-8.

Perry, W., Minassian, A., Lopez, B., Maron, L., Lincoln, A., 2007. Sensorimotor gating deficits in adults with autism. Biol. Psychiatr. 61 (4), 482–486. https://doi.org/10.1016/j.biopsych.2005.09.025.

Pompili, M., Ducci, G., Galluzzo, A., Rosso, G., Palumbo, C., De Berardis, D., 2021. The management of psychomotor agitation associated with schizophrenia or bipolar disorder: a brief review. Int. J. Environ. Res. Publ. Health 18 (8). https://doi.org/10.3390/ijerph18084368.

Powell, S.B., Zhou, X., Geyer, M.A., 2009. Prepulse inhibition and genetic mouse models of schizophrenia. Behav. Brain Res. 204 (2), 282–294. https://doi.org/10.1016/j.bbr.2009.04.021.

Rees, E., Walters, J.T., Chambert, K.D., O'Dushlaine, C., Szatkiewicz, J., Richards, A.L., Kirov, G., 2014. CNV analysis in a large schizophrenia sample implicates deletions at 16p12.1 and SLC1A1 and duplications at 1p36.33 and CGNL1. Hum. Mol. Genet. 23 (6), 1669–1676. https://doi.org/10.1093/hmg/ddt540.

Rohleder, C., Wiedermann, D., Neumaier, B., Drzezga, A., Timmermann, L., Graf, R., Endepols, H., 2016. The functional networks of prepulse inhibition: neuronal connectivity analysis based on FDG-PET in awake and unrestrained rats. Front. Behav. Neurosci. 10, 148. https://doi.org/10.3389/fnbeh.2016.00148.

Rummel, C.K., Gagliardi, M., Ahmad, R., Herholt, A., Jimenez-Barron, L., Murek, V., Ziller, M.J., 2023. Massively parallel functional dissection of schizophrenia-associated noncoding genetic variants. Cell. https://doi.org/10.1016/j.cell.2023.09.015.

Sabik, O.L., Calabrese, G.M., Taleghani, E., Ackert-Bicknell, C.L., Farber, C.R., 2020. Identification of a core module for bone mineral density through the integration of a Co-expression network and GWAS data. Cell Rep. 32 (11), 108145 https://doi.org/10.1016/j.celrep.2020.108145.

Sabik, O.L., Ackert-Bicknell, C.L., Farber, C.R., 2021. A computational approach for identification of core modules from a co-expression network and GWAS data. STAR Protoc 2 (3), 100768. https://doi.org/10.1016/j.xpro.2021.100768.

Santos-Carrasco, D., De la Casa, L.G., 2023. Prepulse inhibition deficit as a transdiagnostic process in neuropsychiatric disorders: a systematic review. BMC Psychol 11 (1), 226. https://doi.org/10.1186/s40359-023-01253-9.

Schizophrenia Working Group of the Psychiatric Genomics, C, 2014. Biological insights from 108 schizophrenia-associated genetic loci. Nature 511 (7510), 421–427. https://doi.org/10.1038/nature13595.

Singh, T., Poterba, T., Curtis, D., Akil, H., Al Eissa, M., Barchas, J.D., Daly, M.J., 2022. Rare coding variants in ten genes confer substantial risk for schizophrenia. Nature 604 (7906), 509–516. https://doi.org/10.1038/s41586-022-04556-w.

Solmi, M., Seitidis, G., Mavridis, D., Correll, C.U., Dragioti, E., Guimond, S., Cortese, S., 2023. Incidence, prevalence, and global burden of schizophrenia - data, with critical appraisal, from the Global Burden of Disease (GBD) 2019. Mol. Psychiatr. https://doi.org/10.1038/s41380-023-02138-4.

Sullivan, P.F., Kendler, K.S., Neale, M.C., 2003. Schizophrenia as a complex trait: evidence from a meta-analysis of twin studies. Arch. Gen. Psychiatr. 60 (12), 1187–1192. https://doi.org/10.1001/archpsyc.60.12.1187.

Swerdlow, N.R., Light, G.A., 2018. Sensorimotor gating deficits in schizophrenia: advancing our understanding of the phenotype, its neural circuitry and genetic substrates. Schizophr. Res. 198, 1–5. https://doi.org/10.1016/j.schres.2018.02.042.

Swerdlow, N.R., Braff, D.L., Geyer, M.A., 2000. Animal models of deficient sensorimotor gating: what we know, what we think we know, and what we hope to know soon. Behav. Pharmacol. 11 (3–4), 185–204. https://doi.org/10.1097/00008877-200006000-00002.

Trubetskoy, V., Pardinas, A.F., Qi, T., Panagiotaropoulou, G., Awasthi, S., Bigdeli, T.B., Schizophrenia Working Group of the Psychiatric Genomics, C, 2022. Mapping genomic loci implicates genes and synaptic biology in schizophrenia. Nature 604 (7906), 502–508. https://doi.org/10.1038/s41586-022-04434-5.

van Dam, S., Vosa, U., van der Graaf, A., Franke, L., de Magalhaes, J.P., 2018. Gene co-expression analysis for functional classification and gene-disease predictions. Briefings Bioinf. 19 (4), 575–592. https://doi.org/10.1093/bib/bbw139.

Velligan, D.I., Rao, S., 2023a. The epidemiology and global burden of schizophrenia. J. Clin. Psychiatry 84 (1). https://doi.org/10.4088/JCP.MS21078COM5.

Velligan, D.I., Rao, S., 2023b. Schizophrenia: salient symptoms and pathophysiology. J. Clin. Psychiatry 84 (1). https://doi.org/10.4088/JCP.MS21078COM7.

Watanabe, K., Taskesen, E., van Bochoven, A., Posthuma, D., 2017. Functional mapping and annotation of genetic associations with FUMA. Nat. Commun. 8 (1), 1826. https://doi.org/10.1038/s41467-017-01261-5.

Watanabe, K., Umicevic Mirkov, M., de Leeuw, C.A., van den Heuvel, M.P., Posthuma, D., 2019. Genetic mapping of cell type specificity for complex traits. Nat. Commun. 10 (1), 3222. https://doi.org/10.1038/s41467-019-11181-1.

Wray, N.R., Wijmenga, C., Sullivan, P.F., Yang, J., Visscher, P.M., 2018. Common disease is more complex than implied by the core gene omnigenic model. Cell 173 (7), 1573–1580. https://doi.org/10.1016/j.cell.2018.05.051.

Xie, Z., Bailey, A., Kuleshov, M.V., Clarke, D.J.B., Evangelista, J.E., Jenkins, S.L., Ma'ayan, A., 2021. Gene set knowledge discovery with enrichr. Curr Protoc 1 (3), e90. https://doi.org/10.1002/cpz1.90.

Yang, Q., Xing, Q., Yang, Q., Gong, Y., 2022. Classification for psychiatric disorders including schizophrenia, bipolar disorder, and major depressive disorder using machine learning. Comput. Struct. Biotechnol. J. 20, 5054–5064. https://doi.org/10.1016/j.csbj.2022.09.014.

Yoon, J.H., Minzenberg, M.J., Ursu, S., Ryan Walter, B.S., Wendelken, C., Ragland, J.D., Carter, C.S., 2008. Association of dorsolateral prefrontal cortex dysfunction with disrupted coordinated brain activity in schizophrenia: relationship with impaired cognition, behavioral disorganization, and global function. Am. J. Psychiatr. 165 (8), 1006–1014. https://doi.org/10.1176/appi.ajp.2008.07060945.

Zebardast, N., Crowley, M.J., Bloch, M.H., Mayes, L.C., Wyk, B.V., Leckman, J.F., Swain, J.E., 2013. Brain mechanisms for prepulse inhibition in adults with Tourette syndrome: initial findings. Psychiatr. Res. 214 (1), 33–41. https://doi.org/10.1016/j.pscychresns.2013.05.009.

Zeighami, Y., Bakken, T.E., Nickl-Jockschat, T., Peterson, Z., Jegga, A.G., Miller, J.A., Hawrylycz, M., 2023. A comparison of anatomic and cellular transcriptome structures across 40 human brain diseases. PLoS Biol. 21 (4), e3002058 https://doi.org/10.1371/journal.pbio.3002058.